Subclass-based Undersampling for Class-Imbalanced Image Classification

Daniel Lehmann and Marc Ebner
Institut für Mathematik und Informatik, Universität Greifswald
Walther-Rathenau-Straße 47, 17489 Greifswald, Germany
{*daniel.lehmann, marc.ebner*}@*uni-greifswald.de*

Keywords: Undersampling, Clustering, CNN.

Abstract: Image classification problems are often class-imbalanced in practice. Such a class imbalance can negatively affect the classification performance of CNN models. A State-of-the-Art (SOTA) approach to address this issue is to randomly undersample the majority class. However, random undersampling can result in an information loss because the randomly selected samples may not come from all distinct groups of samples of the class (subclasses). In this paper, we examine an alternative undersampling approach. Our method undersamples a class by selecting samples from all subclasses of the class. To identify the subclasses, we investigated if clustering of the high-level features of CNN models is a suitable approach. We conducted experiments on 2 real-world datasets. Their results show that our approach can outperform a) models trained on the imbalanced dataset and b) models trained using several SOTA methods addressing the class imbalance.

1 INTRODUCTION

Image classification datasets are often imbalanced in practice. Certain classes contain significantly less frequent samples (minority classes) than the other classes (majority classes). A dataset of images showing healthy plants and plants suffering from a plant disease, for instance, will be imbalanced if the plant disease occurs rarely in nature (minority class: *plant with disease*, majority class: *healthy plant*). A Convolutional Neural Network (CNN) model trained on this dataset may not perform well for images of the less frequent class. During training, the mini-batches mostly contain images of the majority class as they occur more frequently in the data. Hence, the resulting model may only have learned a proper representation of the majority class but not of the minority class.

A State-of-the-Art (SOTA) approach to address this problem is random undersampling (Buda et al., 2018; Lee et al., 2016; More, 2016). Random undersampling balances a dataset by randomly selecting samples of the majority class until the number of picked majority class samples is approximately as high as the number of minority class samples. Then, a model is trained using the minority class samples and the selected majority class samples. A disadvantage of this approach, however, is that it can lose information about the majority class. A class may contain different groups of images (Nguyen et al., 2016; Wei et al., 2015) (subclasses). The ImageNet (Russakovsky et al., 2015) class *baseball*, for instance, can be grouped into images showing a *baseball player* and images showing only the *ball*. If samples from the *baseball* class are randomly selected, then the selected samples may come mostly from only one of the 2 subclasses. As a consequence, a model trained on such an undersampled dataset will not have learned a proper representation of the *baseball* class as it has not seen enough samples from both subclasses.

In this work, we examine an alternative approach to undersample the majority class. Our method selects samples from every subclass. Before we can select any samples, however, we must first find the subclasses within the majority class samples. To identify the subclasses, we use clustering on the high-level features of the CNN model. Using this undersampling method, we state 2 research questions: 1) Is clustering of the high-level image features of a CNN model beneficial for undersampling, and 2) is our approach able to outperform a model trained on the imbalanced dataset as well as models using SOTA methods addressing the class imbalance? Our experiments show that both questions can be answered with yes. Our contributions are as follows: 1) We show that clustering of the high-level image features of a CNN model is beneficial for undersampling, 2) we propose a subclass-based undersampling approach that selects the majority class samples more carefully than a random undersampling, and 3) we show (on 2 real-world datasets) that our method can outperform several SOTA methods addressing the class imbalance.

2 RELATED WORK

To improve random undersampling, various methods have been suggested. Kubat and Matwin (Kubat and Matwin, 1997) introduced one-sided selection, which identifies redundant samples close to a class boundary. Zhang and Mani (Zhang and Mani, 2003) proposed a method that selects samples according to the distance between the majority and minority class samples. Garcia and Herrera (García and Herrera, 2009) suggested an evolutionary undersampling. Majumder et. al. (Majumder et al., 2020) proposed a method based on feature vector angles to pick the samples that contain the most information. Koziarski (Koziarski, 2020a) introduced a radial-based undersampling. Liu et. al. (Liu et al., 2009) proposed EasyEnsemble and BalanceCascade. EasyEnsemble is an ensemble method that picks different subsets of the majority class and trains a model for each of them. BalanceCascade, in contrast, trains a model sequentially. In each iteration, the correctly classified majority class samples are removed from the training set. However, the methods most similar to ours are cluster-based (Agrawal et al., 2015; Sowah et al., 2016; Tsai et al., 2019; Yen and Lee, 2009) and hashing-based undersampling (Ng et al., 2020). Cluster-based undersampling attempts to find clusters in the dataset and then selects samples from each identified cluster. Hashing-based undersampling, in contrast, uses hashing to divide the majority class into subspaces. However, both methods have been suggested for tabular data and can not be used for image data directly. Our method, in contrast, is applied to images used for CNN training. We investigated if clustering of high-level image features can be used for undersampling.

Besides undersampling, several other approaches have been proposed to address model training using a class-imbalanced dataset. A widely used approach is oversampling, which creates additional samples for the minority class to balance the dataset. A simple method to oversample a class is to duplicate randomly selected samples of that class (More, 2016). Singh and Dhall (Singh and Dhall, 2018) improved this method by not selecting samples randomly for duplication but based on the distance of a sample to its cluster centroid. Besides duplicating samples, various methods have been suggested to oversample a minority class by creating synthetic samples for that class (Ando and Huang, 2017; Chawla et al., 2002; Hao et al., 2020; Mullick et al., 2019). Shen et. al. (Shen et al., 2016) do not create any samples but uniformly populate the mini-batches with samples from all classes during model training. Kozarski (Koziarski, 2020b) introduced a method that combines oversampling and undersampling. Furthermore, there has been work that addresses the class imbalance by introducing a special loss function (Cao et al., 2019; Dong et al., 2017; More, 2016; Sarkar et al., 2020), a balanced group softmax (Li et al., 2020), dynamic sampling (Pouyanfar et al., 2018), dynamic curriculum learning (Wang et al., 2019), cost-sensitive learning (Khan et al., 2015), a local embedding (Huang et al., 2016) or category centers (Zhang et al., 2018). Category centers are also used in high-level image feature space. However, the centers are exploited for the classification process and not to undersample the dataset as our method does.

3 METHOD

Our undersampling method can be applied to multi-class imbalanced image datasets containing several majority classes. To balance such a dataset, our method must be applied to each majority class separately. Thus, in order to explain our method, we consider a two-class imbalanced dataset containing only one majority class in the following without losing generality. We undersample the majority class in 2 stages. First, we identify the subclasses of the majority class (as shown in steps 1 to 4 in Figure 1). Second, we select representative samples from each identified subclass (as shown in step 5 in Figure 1). The selected majority class samples and all minority class samples form the new undersampled dataset. We describe both stages in more detail below.

In order to identify subclasses of the majority class C, we use a method similar to that suggested by Nguyen et. al. (Nguyen et al., 2016). However, Nguyen et. al. introduced their method to visualize multifaceted features learned by a CNN. We adapted their method to find representative samples of a class for undersampling that class. First, we train an initial model f_0 using the imbalanced training set (X,Y). The resulting model f_0 may not perform well for the minority class as it is underrepresented in the data. We assume, however, the model f_0 learns at least a sufficient representation of the majority class C. After we trained the model f_0, we use this model to extract features from each image x^C of the majority class C. We assume C has N_C samples x^C in the training set

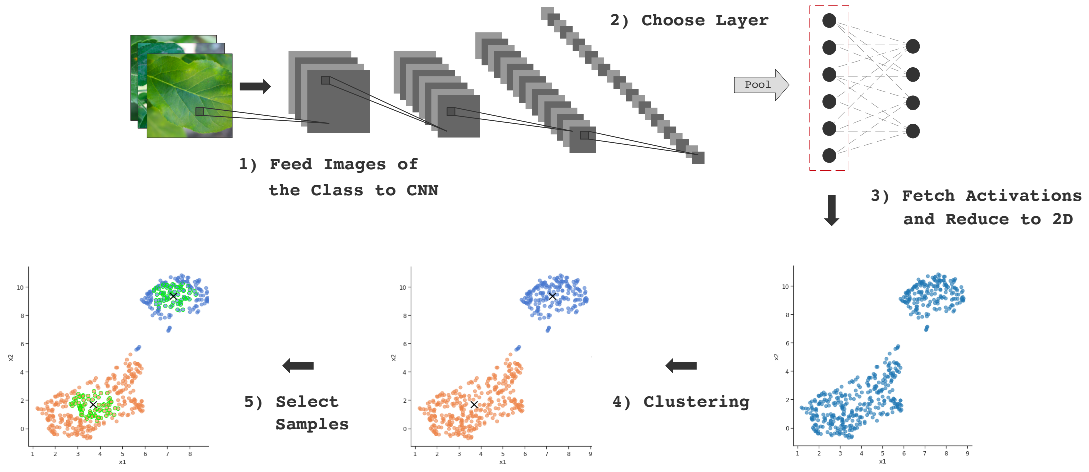

2) Choose Layer
Pool
1) Feed Images of the Class to CNN
3) Fetch Activations and Reduce to 2D
5) Select Samples
4) Clustering

Figure 1: Our method: 1) Feed majority class images into the initial CNN model (trained on the imbalanced dataset), 2) choose a layer from which to fetch activations, 3) fetch activations of the images at the chosen layer and reduce activations to 2D, 4) find clusters in the activations and 5) select samples from each identified cluster.

(X,Y). In order to extract the features, we feed all N_C images x^C into model f_0. At a certain layer L, we fetch the layer activations of each image x^C. The activations represent the features that layer L extracts from the images x^C. Which layer to pick depends on the classification problem to solve. It is important, however, to choose one of the last layers of the CNN (i.e., closer to the output layer). The last layers of a CNN extract high-level features (e.g., object parts), while the earlier layers extract low-level features (e.g., edges, simple shapes) as shown by Zeiler and Fergus (Zeiler and Fergus, 2014). In order to identify subclasses representing different semantic concepts (e.g., the subclass *baseball player* and the subclass *ball* from the ImageNet class *baseball*), we must use the high-level features from one of the last network layers as only these features are characteristic for the different semantic concepts. If the chosen layer is a convolutional layer, the fetched activations of each image x^C will be in cube form. To convert the activations to vector form, we flatten the activations. If the chosen layer is a linear layer, however, the fetched activations will be in vector form already, and we do not need to flatten them. In either case, we receive N_C feature vectors a_{x^C} (one from each image x^C) of length M^L. Then, we concatenate all N_C vectors a_{x^C} to a feature matrix A^C of size $N_C \times M^L$.

In the data of the matrix A^C, we try to find clusters representing different subclasses of C. Before we can apply clustering on the data, however, we need to reduce the dimensions of the feature matrix A^C from $N_C \times M^L$ down to $N_C \times 2$. This preprocessing step is necessary as clustering is usually more difficult to apply in high dimensions (Chen et al., 2019). First, we normalize A^C by subtracting the mean and then dividing by the standard deviation (prerequisite for dimensionality reduction). Then, we project A^C from $N_C \times M^L$ down to $N_C \times 50$ using PCA (Pearson, 1901) followed by a second reduction from $N_C \times 50$ down to $N_C \times 2$ using UMAP (McInnes et al., 2018). As a result, we receive the projected features matrix $p(A^C)$ of size $N_C \times 2$. The reason why we use PCA and UMAP combined is that A^C is usually too large to directly apply a non-linear dimensionality reduction technique such as UMAP. On the other hand, using only a linear dimensionality reduction (such as PCA) did not result in a sufficient data representation in our experiments. Thus, we use a combination of both techniques. A similar approach was also suggested by Ngyuen et. al. (Nguyen et al., 2016). Finally, we apply k-Means clustering (MacQueen, 1967) on $p(A^C)$ to identify clusters in the feature data. To find the parameter k, we apply k-Means multiple times using different k (values: 2-9) and compute the Silhouette score (Rousseeuw, 1987) of the resulting clusters for each k. The Silhouette score is an evaluation metric that measures the cluster quality using the mean inter-cluster and mean intra-cluster distance (range: between -1 and 1, a higher score means a better cluster quality). As Chen et. al. (Chen et al., 2019) pointed out, this score works well for evaluating clusters in the layer activations of a CNN. Thus, we choose the k that obtained the best Silhouette score. As a result, we receive $1,\ldots,k$ clusters, which represent the potential subclasses of the majority class.

After identifying $1,\ldots,k$ clusters in $p(A^C)$, we select a certain number of representative samples $x^C_{u_k}$ from each cluster $1,\ldots,k$. For instance, if we need to select 100 majority class samples, and we found 2 clusters, we will select 50 samples from each identified cluster. In order to select the samples from each cluster, we consider 2 options: a) We select the samples from each cluster that are closest to their cluster center, and b) we select the samples from each cluster that are farthest from their cluster center (excluding outliers). The most representative samples of a cluster should be samples closest to their cluster center. Therefore, we chose to examine option a). On the other hand, however, the samples closest to a cluster center may be quite similar if these samples are close to each other as well. We would like to select samples that are as unique as possible when undersampling the data. Thus, we also examine option b) by selecting the samples of a cluster that are most far away from their cluster center. In order to avoid selecting outliers (e.g., noise, mislabeled samples), however, we only consider the 80th percentile of all the samples of a cluster. After selecting the samples $x^{C}_{u^k}$ from each cluster $1,...,k$ using one of the 2 options, we merge these samples together with all minority class samples to obtain the undersampled dataset (X^u, Y^u). This dataset can be used to train a new model f_u.

4 EXPERIMENTS

4.1 Experimental Setup

We conducted several experiments to test our method described in section 3. For each experiment, we executed the following steps: 1) Training an initial model, 2) selecting a layer of that model, 3) feeding all training images of the class that should be undersampled to the model and fetching their activations at the selected layer, 4) finding clusters in the fetched activations, 5) picking a certain number of samples from each cluster, 6) using the picked samples and all training images from the other classes that should not be undersampled as the new training set, 7) training a model using the new undersampled training set, and 8) comparing this model to a model trained on the imbalanced training set (baseline) and to models trained using SOTA methods addressing the class imbalance (e.g., through random undersampling, oversampling, a class-weighted loss) with respect to their performance on the test set.

For our experiments we used the datasets from 2 image classification competitions hosted on the data science platform Kaggle: a) The Plant Pathology 2020[1] competition (Thapa et al., 2020) and b) the Fisheries Monitoring[2] competition. The Plant Pathology dataset has 4 classes. One of the classes contains significantly fewer images than the other classes. The Fisheries Monitoring dataset, in contrast, has 8 classes. One of the classes contains significantly more images than the other classes.

We used the same training setup for all of our models. Except for our experiments in section 4.4, we chose a ResNet50 (He et al., 2016) as model architecture. All models were pretrained on ImageNet (Russakovsky et al., 2015). We removed the output layer (for the ImageNet classes) and replaced it with the following new layers: A combination of an adaptive average pooling layer and an adaptive max pooling layer (output of both are concatenated) - BatchNorm - Dropout ($p = 0.25$) - Linear layer (size: 512) - ReLU - BatchNorm - Dropout ($p = 0.5$) - Linear output layer. Each model was fine-tuned using a discriminative fine-tuning strategy (Howard and Ruder, 2018) in a two-stage process. First, we fine-tuned only the initial weights of the new layers (which we added) for 3 epochs. Then, we fine-tuned the weights of all layers of the network for 8 more epochs. The learning rate was set to an initial value of 0.01 and was then adjusted over the course of training via a cyclical learning rate schedule (Smith, 2017). We used mixed precision training (Micikevicius et al., 2018) to be able to set the batch size to 25. For the Plant Pathology data, we adopted all data augmentation techniques from the original winner[3] of the corresponding competition (brightness, contrast, blur, shift, scale, rotation, horizontal and vertical flip). For the Fisheries Monitoring data, we used the same data augmentation techniques except for the vertical flip. Unlike the Plant Pathology images, the images of the Fisheries Monitoring dataset were always taken from the same vertical orientation. All images of both datasets were resized to 224×224 before training.

Each model was evaluated using the Kaggle submission system. The submission system evaluates the Plant Pathology competition using the ROC AUC[1] metric, while it evaluates the Fisheries Monitoring competition using the multi-class logarithmic loss[2] (LogLoss). Kaggle splits the test set of a competition into 2 parts: A public and a private test set. While the competition is active, the submission system only shows how a model performed on the public test set. When the competition is over, the evaluation score on the private test set will be visible as well. The user with the best score on the private test set wins the competition. As the Plant Pathology and the Fish-

[1]https://www.kaggle.com/c/plant-pathology-2020-fgvc7

[2]https://www.kaggle.com/c/the-nature-conservancy-fisheries-monitoring

[3]https://github.com/alipay/cvpr2020-plant-pathology

Table 1: Comparison of our method (selecting closest/farthest samples to cluster center) to the baseline (imbalanced dataset) and random undersampling on the Plant Pathology data. All models were trained over 6 random seeds. The results are reported as median ROC AUC scores (a higher value is better) and standard deviations (std) over the 6 seeds.

Method	Undersampled Class	ROC AUC	
		median	*std*
Baseline	-	0.9387	0.0045
Random Undersampling	healthy	0.9375	0.0086
	rust	0.9187	0.0092
	scab	0.9377	0.0024
	healthy, rust, scab	0.9068	0.0233
Ours (closest)	healthy	0.9391	0.0058
	rust	0.9171	0.0069
	scab	**0.9425**	0.0088
	healthy, rust, scab	0.8909	0.0166
Ours (farthest)	healthy	0.9353	0.0059
	rust	0.9183	0.0098
	scab	0.9369	0.0080
	healthy, rust, scab	0.9004	0.0054

eries Monitoring competition are both not active anymore, the evaluation scores on the private test set are already available for both competitions. Thus, we use the scores on the private test set to evaluate our models as these are crucial for winning the competitions.

4.2 Selecting Closest Samples

We conducted an experiment to test whether our undersampling approach using the closest samples to each identified cluster center (as described in section 3) is able to improve model performance. As the Plant Pathology dataset contains 3 majority classes (*rust*, *scab* and *healthy*), we examined 4 different undersampling strategies: 1) Undersampling of the *healthy* class only (from 516 to 100 samples), 2) undersampling of the *rust* class only (from 622 to 100 samples), 3) undersampling of the *scab* class only (from 592 to 100 samples) and, 4) undersampling of the *healthy*, *rust* and *scab* class (to 100 samples per class). To be able to find clusters in the data of a majority class, our method requires choosing a layer whose activations should be used for clustering. We considered the last 3 layers before the output layer of the network. Among these 3 layers, we chose the layer whose activations reached the best Silhouette score. For *rust* and *healthy*, we obtained the best Silhouette score using the activations of the adaptive pooling layer (concatenation of average and max pooling), while for *scab* the last linear layer before the output layer resulted in the best Silhouette score. For each class, we picked the same number of samples from each identified cluster. For instance, we found 2 clusters in the data of the *healthy* class. Therefore, we picked 50 samples closest to each cluster center to obtain 100 samples in total for that class. As a result, we received the following datasets: a) One undersampled dataset from our method for each strategy 1) - 4), b) the baseline (imbalanced dataset) and c) 6 randomly undersampled datasets (More, 2016) (using a different random seed each time for the random sampling) for each strategy 1) - 4). With each of these datasets, we trained 6 models using a different random seed each time and report the median test performance over the 6 models. The results are shown in Table 1.

The Fisheries Monitoring dataset contains 1 majority class (*ALB* class). As a result, we undersampled only this class (from 1719 to 734 samples). Again, we selected the same number of samples from each identified cluster. We obtained the best Silhouette score using the activations of the last ResNet50 layer before the newly added layers. Thus, we used these layer activations to undersample the class. Then, we trained a model (1 seed) using a) the dataset undersampled by our method (using the closest samples), b) the baseline (imbalanced dataset), and c) 5 randomly undersampled datasets (More, 2016) (using a different random seed each time for the random sampling). The results of our experiment for the Fisheries Monitoring data are shown in Table 2.

4.3 Selecting Farthest Samples

In another experiment, we tested if our undersampling approach using the farthest samples from each identified cluster center is able to improve model performance. The experimental setup was the same as in section 4.2, except for the method how to pick the samples. Instead of selecting the closest samples to each cluster center, we undersampled the data by

Table 2: Comparison of our method to the baseline (imbalanced dataset) and random undersampling (median over 5 random samplings) on the Fisheries Monitoring data (undersampling of class *ALB*). The results are reported as multi-class logarithmic loss (a lower value is better).

Method	LogLoss
Baseline	5.7333
Random Undersampling	4.0771
Ours (closest)	**3.8657**
Ours (farthest)	3.9302

picking the farthest samples from each cluster center, as described in section 3. The results of the experiment for the Plant Pathology data are shown in Table 1, and the results of the experiment for the Fisheries Monitoring data are shown in Table 2. In contrast to section 4.2, however, we obtained the best Silhouette score for the Fisheries Monitoring dataset using the activations of the adaptive pooling layer. Thus, we used these layer activations for undersampling.

4.4 Other CNN Architectures

In our experiments in section 4.2 and section 4.3, we used a pretrained ResNet50 for all our models, as described in section 4.1. To examine how our undersampling approach performs using other CNN architectures, we conducted additional experiments for the *healthy* class (516 samples) of the Plant Pathology data. The experimental setup was the same as for the experiments in section 4.2 and section 4.3, except for the CNN architecture. We examined 2 additional architectures: a) DenseNet121 (Huang et al., 2017) and b) VGG16 (Simonyan and Zisserman, 2015) (with BatchNorm (Ioffe and Szegedy, 2015)). A model was trained (1 seed) for each architecture using a) the dataset undersampled by our method (to 100 samples), b) the baseline (imbalanced dataset), and c) 5 randomly undersampled datasets (More, 2016) (to 100 samples using a different random seed each time for the random sampling). The results of the experiment are shown in Table 3.

4.5 Comparison to SOTA Methods

In our experiments in section 4.2, 4.3 and 4.4 we only compared our method to the baseline (imbalanced dataset) and random undersampling (More, 2016). In another experiment, we examined how our method performs in comparison to other SOTA methods addressing data imbalance applied to the Plant Pathology dataset: a) oversampling (More, 2016) of the minority class (*multiple diseases* class, 91 samples) and b) a training approach using a class-weighted loss function (More, 2016). For oversampling, we tested 2

Table 3: Comparison of our method to the baseline (imbalanced dataset) and random undersampling (median over 5 random samplings) with respect to different CNN architectures on the Plant Pathology data (undersampling of class *healthy*). The results are reported as ROC AUC scores (a higher value is better).

Method	CNN Arch.	ROC AUC
Baseline	VGG16	0.9435
Rand. Undersamp.		0.9404
Ours (closest)		**0.9447**
Ours (farthest)		0.9322
Baseline	DenseNet121	0.9461
Rand. Undersamp.		0.9384
Ours (closest)		0.9294
Ours (farthest)		**0.9465**

approaches: 1) duplicating the minority class samples 2 times (resulting in 182 samples), and b) duplicating the minority class samples 6 times (resulting in 546 samples). For the class-weighted loss function, we set the weights for each class according to the fraction of samples of that class among the total number of samples of the Plant Pathology dataset. Moreover, we tested 2 additional configurations for undersampling the *healthy* class using our method. First, besides selecting the closest samples to each cluster center and selecting the farthest samples from each cluster center, we also selected samples from each cluster randomly. Second, besides undersampling the *healthy* class from 516 to 100 samples, we also undersampled the *healthy* class from 516 to 250 samples. We trained a model (1 seed) for each method. The results of the experiment are shown in Table 4.

Table 4: Comparison of our method (undersampling of class *healthy*) to the baseline (imbalanced dataset), random undersampling, oversampling, and a class-weighted loss approach on the Plant Pathology data. The results are reported as ROC AUC scores (a higher value is better).

Method	ROC AUC
Baseline	0.9343
Class-Weighted Loss	0.9466
Oversampling (182 samples)	0.9469
Oversampling (546 samples)	0.9268
Rand. Undersamp. (100 samples)	0.9370
Ours (closest, 100 samples)	0.9451
Ours (farthest, 100 samples)	0.9301
Ours (random, 100 samples)	0.9377
Rand. Undersamp. (250 samples)	0.9474
Ours (closest, 250 samples)	0.9488
Ours (farthest, 250 samples)	0.9453
Ours (random, 250 samples)	**0.9551**

5 CONCLUSION

In section 1, we stated 2 research questions: 1) Is clustering of the high-level image features of a CNN model beneficial for undersampling, and 2) is our approach able to outperform a model trained on the imbalanced dataset as well as models using SOTA methods addressing the class imbalance? Our experiments (section 4) show that our method is able to obtain a better performance than the baseline and a random undersampling. Moreover, our method is also able to surpass the performance of other SOTA methods addressing data imbalance (oversampling, class-weighted loss). Selecting the closest samples to each cluster center for undersampling the majority class performed best in most cases in our experiments. However, there were also cases in which selecting the farthest samples from each cluster center or a random cluster sample selection reached a better performance. As a result, we have shown that a subclass-based undersampling is able to surpass the performance of a model trained on the imbalanced dataset (baseline) and models trained using SOTA methods addressing the class imbalance. This could also be helpful for other research areas. In medical imaging, for instance, datasets are frequently imbalanced as well (Larrazabal et al., 2020; Reza and Ma, 2018). Furthermore, datasets in practice often contain label noise (Algan and Ulusoy, 2021; Xiao et al., 2015), i.e., some images of a dataset were inadvertently mislabeled. In future work, it could be investigated if we can identify such noise using our method.

REFERENCES

Agrawal, A., Viktor, H. L., and Paquet, E. (2015). Scut: Multi-class imbalanced data classification using smote and cluster-based undersampling. In *IC3K*, volume 1, pages 226–234, Lisbon, Portugal. IEEE.

Algan, G. and Ulusoy, I. (2021). Image classification with deep learning in the presence of noisy labels: A survey. *Knowledge-Based Systems*, 215:106771.

Ando, S. and Huang, C. Y. (2017). Deep over-sampling framework for classifying imbalanced data. In Ceci, M., Dzeroski, S., Vens, C., Todorovski, L., and Hollmen, J., editors, *ECML PKDD*, Lecture Notes in CS, pages 770–785. Springer.

Buda, M., Maki, A., and Mazurowski, M. A. (2018). A systematic study of the class imbalance problem in convolutional neural networks. *Neural Networks*, 106:249–259.

Cao, K., Wei, C., Gaidon, A., Arechiga, N., and Ma, T. (2019). Learning imbalanced datasets with label-distribution-aware margin loss. In Wallach, H., Larochelle, H., Beygelzimer, A., d'Alché-Buc, F., Fox, E., and Garnett, R., editors, *Adv Neural Inf Process Syst*, volume 32, Vancouver, CA. CAI.

Chawla, N. V., Bowyer, K. W., Hall, L. O., and Kegelmeyer, W. P. (2002). Smote: Synthetic minority over-sampling technique. *Journal of Artif Int Res*, 16(1):321–357.

Chen, B., Carvalho, W., Baracaldo, N., Ludwig, H., Edwards, B., Lee, T., Molloy, I., and Srivastava, B. (2019). Detecting backdoor attacks on deep neural networks by activation clustering. In Espinoza, H., hÉigeartaigh, S. Ó., Huang, X., Hernández-Orallo, J., and Castillo-Effen, M., editors, *Workshop on SafeAI@AAAI*, volume 2301 of *CEUR Workshop*, Honolulu, HI, USA. ceur-ws.org.

Dong, Q., Gong, S., and Zhu, X. (2017). Class rectification hard mining for imbalanced deep learning. In *ICCV*, pages 1869–1878, Venice, Italy. IEEE.

García, S. and Herrera, F. (2009). Evolutionary undersampling for classification with imbalanced datasets: Proposals and taxonomy. *Evol Comput*, 17(3):275–306.

Hao, J., Wang, C., Zhang, H., and Yang, G. (2020). Annealing genetic gan for minority oversampling. *ArXiv*, abs/2008.01967.

He, K., Zhang, X., Ren, S., and Sun, J. (2016). Deep residual learning for image recognition. In *CVPR*, pages 770–778, Las Vegas, NV, USA. IEEE.

Howard, J. and Ruder, S. (2018). Universal language model fine-tuning for text classification. In *Proc of the ACL*, pages 328–339, Melbourne, Australia. ACL.

Huang, C., Li, Y., Loy, C. C., and Tang, X. (2016). Learning deep representation for imbalanced classification. In *CVPR*, pages 5375–5384, Las Vegas, NV, USA. IEEE.

Huang, G., Liu, Z., Van Der Maaten, L., and Weinberger, K. Q. (2017). Densely connected convolutional networks. In *CVPR*, pages 2261–2269, Honolulu, HI, USA. IEEE.

Ioffe, S. and Szegedy, C. (2015). Batch normalization: Accelerating deep network training by reducing internal covariate shift. In Bach, F. and Blei, D., editors, *ICML*, volume 37 of *Proc Mach Learn Res*, page 448–456, Lille, France. PMLR.

Khan, S. H., Hayat, M., Bennamoun, M., Sohel, F., and Togneri, R. (2015). Cost sensitive learning of deep feature representations from imbalanced data. *ArXiv*, abs/1508.03422.

Koziarski, M. (2020a). Radial-based undersampling for imbalanced data classification. *Pattern Recognition*, 102:107262.

Koziarski, M. (2020b). Two-stage resampling for convolutional neural network training in the imbalanced colorectal cancer image classification. *ArXiv*, abs/2004.03332.

Kubat, M. and Matwin, S. (1997). Addressing the curse of imbalanced training sets: One-sided selection. In *ICML*, pages 179–186. Morgan Kaufmann.

Larrazabal, A. J., Nieto, N., Peterson, V., Milone, D. H., and Ferrante, E. (2020). Gender imbalance in medical imaging datasets produces biased classifiers for computer-aided diagnosis. *Proc National Academy of Sciences*, 117(23):12592–12594.

Lee, H., Park, M., and Kim, J. (2016). Plankton classification on imbalanced large scale database via convolutional neural networks with transfer learning. In *ICIP*, pages 3713–3717, Phoenix, AZ, USA. IEEE.

Li, Y., Wang, T., Kang, B., Tang, S., Wang, C., Li, J., and Feng, J. (2020). Overcoming classifier imbalance for long-tail object detection with balanced group softmax. In *CVPR*, pages 10991–11000.

Liu, X.-Y., Wu, J., and Zhou, Z.-H. (2009). Exploratory undersampling for class-imbalance learning. *Trans. Sys. Man Cyber. Part B*, 39(2):539–550.

MacQueen, J. B. (1967). Some methods for classification and analysis of multivariate observations. In Cam, L. M. L. and Neyman, J., editors, *Berkeley Symp on Math Stat and Prob*, volume 1, pages 281–297. Univ of Calif Press.

Majumder, A., Dutta, S., Kumar, S., and Behera, L. (2020). A method for handling multi-class imbalanced data by geometry based information sampling and class prioritized synthetic data generation (gicaps). *ArXiv*, abs/2010.05155.

McInnes, L., Healy, J., and Melville, J. (2018). UMAP: Uniform manifold approximation and projection for dimension reduction. *ArXiv*, abs/1802.03426.

Micikevicius, P., Narang, S., Alben, J., Diamos, G., Elsen, E., Garcia, D., Ginsburg, B., Houston, M., Kuchaiev, O., Venkatesh, G., and Wu, H. (2018). Mixed precision training. In *ICLR*, Vancouver, CA.

More, A. (2016). Survey of resampling techniques for improving classification performance in unbalanced datasets. *ArXiv*, abs/1608.06048.

Mullick, S. S., Datta, S., and Das, S. (2019). Generative adversarial minority oversampling. In *ICCV*, pages 1695–1704, Seoul, South Korea. IEEE.

Ng, W. W., Xu, S., Zhang, J., Tian, X., Rong, T., and Kwong, S. (2020). Hashing-based undersampling ensemble for imbalanced pattern classification problems. *Transactions on Cybernetics*.

Nguyen, A., Yosinski, J., and Clune, J. (2016). Multifaceted feature visualization: Uncovering the different types of features learned by each neuron in deep neural networks. *ArXiv*, abs/1602.03616.

Pearson, K. (1901). LIII. On lines and planes of closest fit to systems of points in space. *London, Edinburgh Dublin Philos Mag J Sci*, 2(11):559–572.

Pouyanfar, S., Tao, Y., Mohan, A., Tian, H., Kaseb, A. S., Gauen, K., Dailey, R., Aghajanzadeh, S., Lu, Y. H., Chen, S. C., and Shyu, M. L. (2018). Dynamic sampling in convolutional neural networks for imbalanced data classification. In *MIPR*, Proc MIPR 2018, pages 112–117. Inst Electrical and Electronics Engineers Inc.

Reza, M. S. and Ma, J. (2018). Imbalanced histopathological breast cancer image classification with convolutional neural network. In *ICSP*, pages 619–624. IEEE.

Rousseeuw, P. J. (1987). Silhouettes: A graphical aid to the interpretation and validation of cluster analysis. *J. Comput. Appl. Math.*, 20(1):53–65.

Russakovsky, O., Deng, J., Su, H., Krause, J., Satheesh, S., Ma, S., Huang, Z., Karpathy, A., Khosla, A., Bernstein, M., Berg, A. C., and Fei-Fei, L. (2015). Imagenet large scale visual recognition challenge. *IJCV*, 115(3):211–252.

Sarkar, D., Narang, A., and Rai, S. (2020). Fed-focal loss for imbalanced data classification in federated learning. *ArXiv*, abs/2011.06283.

Shen, L., Lin, Z., and Huang, Q. (2016). Relay backpropagation for effective learning of deep convolutional neural networks. In Leibe, B., Matas, J., Sebe, N., and Welling, M., editors, *ECCV*, volume 9911 of *Lecture Notes in CS*, pages 467–482. Springer.

Simonyan, K. and Zisserman, A. (2015). Very deep convolutional networks for large-scale image recognition. In Bengio, Y. and LeCun, Y., editors, *ICLR*, San Diego, CA, USA.

Singh, N. D. and Dhall, A. (2018). Clustering and learning from imbalanced data. *ArXiv*, abs/1811.00972.

Smith, L. N. (2017). Cyclical learning rates for training neural networks. In *WACV*, pages 464–472. IEEE.

Sowah, R. A., Agebure, M. A., Mills, G. A., Koumadi, K. M., and Fiawoo, S. Y. (2016). New cluster undersampling technique for class imbalance learning. *Int Journal of Mach Learning and Computing*, 6(3):205.

Thapa, R., Zhang, K., Snavely, N., Belongie, S., and Khan, A. (2020). The plant pathology challenge 2020 data set to classify foliar disease of apples. *Appl in Plant Sciences*, 8(9):e11390.

Tsai, C.-F., Lin, W.-C., Hu, Y.-H., and Yao, G.-T. (2019). Under-sampling class imbalanced datasets by combining clustering analysis and instance selection. *Information Sciences*, 477:47–54.

Wang, Y., Gan, W., Yang, J., Wu, W., and Yan, J. (2019). Dynamic curriculum learning for imbalanced data classification. In *ICCV*, pages 5016–5025, Seoul, South Korea. IEEE.

Wei, D., Zhou, B., Torrabla, A., and Freeman, W. (2015). Understanding intra-class knowledge inside CNN. *ArXiv*, abs/1507.02379.

Xiao, T., Xia, T., Yang, Y., Huang, C., and Wang, X. (2015). Learning from massive noisy labeled data for image classification. In *CVPR*, pages 2691–2699, Boston, MA, USA. IEEE.

Yen, S.-J. and Lee, Y.-S. (2009). Cluster-based undersampling approaches for imbalanced data distributions. *Expert Systems with Applications*, 36(3):5718–5727.

Zeiler, M. D. and Fergus, R. (2014). Visualizing and understanding convolutional networks. In Fleet, D., Pajdla, T., Schiele, B., and Tuytelaars, T., editors, *ECCV*, number PART 1 in Lecture Notes in CS, pages 818–833, Zurich, CH. Springer.

Zhang, J. and Mani, I. (2003). kNN approach to unbalanced data distributions: A case study involving information extraction. In *Proc ICML Workshop on Learning from Imbalanced Datasets*, volume 126.

Zhang, Y., Shuai, L., Ren, Y., and Chen, H. (2018). Image classification with category centers in class imbalance situation. In *YAC*, pages 359–363.